Paper No.
07243

NACE INTERNATIONAL CORROSION 2007 CONFERENCE & EXPO

LOCALIZED CORROSION SUSCEPTIBILITY OF COPPER-NICKEL ALLOYS IN CHLORIDE CONTAINING ENVIRONMENTS

Marta A. Jakab
Southwest Research Institute
6220 Culebra Road
San Antonio, TX, 78238

Narasi Sridhar
Southwest Research Institute
6220 Culebra Road
San Antonio, TX, 78238

Andre M. Anderko
OLI Systems Inc.
108 American Road
Morris Plains, NJ, 07950

ABSTRACT

Under alkaline conditions, copper-nickel alloys are covered by passive oxide films containing Cu and Ni oxides. In chloride ion containing environments, they are therefore susceptible to localized corrosion. In this paper, the susceptibility of selected Cu-Ni alloys (UNS C70600, UNS C71500 and UNS N04400) to localized corrosion was investigated by measuring the crevice stabilization and repassivation potentials (E_{crev} and E_{rcrev}, respectively) in alkaline sodium chloride solutions. Correlations between environmental variables, such as chloride ion concentration, pH and temperature and E_{crev}, as well as E_{rcrev} were established. It was found that: (i) E_{crev} and E_{rcrev} decrease with increasing chloride ion concentration; (ii) there is a linear relationship between E_{crev} and E_{rcrev} and the logarithm of chloride ion concentration; (iii) E_{rcrev} does not depend on the solution pH; (iv) there is a complex relationship between E_{crev} and E_{rcrev} and the alloy composition as well as the temperature. The electrochemical properties of the selected alloys were also investigated in synthetic seawater with and without the presence of free chlorine. It was found that the pitting and repassivation potentials in synthetic seawater are strongly dependent on the alloy composition. The presence of free chlorine did not significantly affect the cathodic reaction kinetics. It, however, increased the corrosion potential and changed the corrosion morphology.

Keywords: Cu-Ni alloys, corrosion, crevice, repassivation potential, corrosion potential, synthetic seawater

INTRODUCTION

Copper-nickel alloys are widely used in both marine and offshore environments, as, for example, piping or heat exchanger material in marine environments, or for vessels, pipelines, filters and valves in the chemical and process industries as well as for heat exchangers in power plants. These alloys are known for their excellent corrosion resistance and good resistance to biofouling[1]. The environment (e.g., oxygen content, solution composition, flow rate), however, significantly affects their corrosion rate.

Under alkaline conditions, these alloys are covered by passive oxide films containing Cu and Ni oxides[2-7], while under acidic conditions, they show active dissolution behavior[2,8]. The pH value, where the active-passive transition occurs depends on the alloy composition; it decreases with increasing nickel content[9].

In general, the corrosion resistance of Cu-Ni alloys increases with increasing nickel content up to approximately 30 weight %, then it remains constant[5] or slightly decreases[2]. Nickel additions are thought to have a beneficial effect on the passivation reaction, and the Ni was found to be incorporated in the oxide layer[6]. The oxide layer is usually enriched in Ni, and the degree of Ni enrichment increases with increasing Ni content[6].

In alkaline, chloride ion containing environments, the Cu-Ni alloys are susceptible to localized corrosion due to the breakdown of the oxide layer caused by chloride ions[10,11]. The extent of localized corrosion was found to be a function of the structure, composition and thickness of the passive film[12]. During the breakdown of the passive layer, the chloride ions are incorporated into the oxide, which modifies the oxide lattice. The breakdown of the passive layer can be described by the point defect model[10]. It is believed that as the Cl^- ions replace the O^{2-} ions in the lattice, the cation diffusion is enhanced through the oxide layer and the charge imbalance caused by the ion substitution is neutralized by the ejection of a Cu^+ ion into the solution creating a cation vacancy according to Equation 1[10]:

$$Cu^{+}_{metal} + O^{2-}_{oxide} + Cl^{-}_{electrolyte} + 2\,H^{+}_{electrolyte} = Cu^{+}_{electrolyte} + Cl^{-}_{oxide} + H_2O \qquad (1)$$

The copper ion dissolution causes the formation of a porous film over the dissolution site weakening the passive layer[13].

Only limited information is available regarding crevice corrosion of Cu-Ni alloys. It is, however, very important because of the tendency of deposit formation under stagnant conditions in seawater that contains high levels of suspended particles[14]. Crevice corrosion of Cu-Ni alloys readily occurs under these deposits, especially in the presence of sulfate reducing bacteria (SRB). The role of crevice chemistry in the initiation, stabilization, and repassivation of crevice corrosion has not been reported for these alloys.

In order to control biofouling in seawater, chlorination is often used. The recommended residual free chlorine level is between 0.2 and 0.5 ppm[14]. In some cases, it was found that the corrosion resistance of the Cu-Ni alloys increased in the presence of low concentrations of Cl_2[15,16]. In general, it was observed that chlorine concentrations within the recommended range do not have any negative effect on the corrosion of Cu-Ni alloys, however, free chlorine concentrations higher than 0.5 ppm may have adverse effects, thus should be avoided[14].

The susceptibility to localized corrosion can be predicted by measuring the repassivation potential in chloride containing environments. The repassivation potential is the potential below which localized corrosion is not initiated. It has been shown that the repassivation potential of deep pits is independent of prior pit growth in many alloys[17], thus, it can be used in long-term prediction of localized corrosion[17]. Localized corrosion occurs when the corrosion potential exceeds the repassivation potential in the given environment[18]. Therefore, both the corrosion and repassivation potentials need to be calculated in an effort to predict and model the localized corrosion of an alloy system[18]. A thermodynamic-electrochemical model can be used to calculate these potentials[19,20]. The model, however, contains several parameters that need to be determined from experimental polarization and corrosion rate data.

The goal of this study is to determine how the crevice stabilization and repassivation potentials of three, selected Cu-Ni alloys, namely, CDA 706 (UNS C70600), CDA 715 (UNS C71500) and M400 (UNS N04400), depend on the environmental variables, such as chloride ion concentration, solution pH and temperature. These results will then be used in a thermodynamic-electrochemical model to predict the localized corrosion susceptibility of Cu-Ni alloys in different chemical environments. Moreover, this study investigates the effect of free chlorine concentration on the electrochemical properties of the same alloys in synthetic seawater without the presence of the biological medium.

EXPERIMENTAL PROCEDURE

Materials

The experiments were conducted using UNS C70600, UNS C71500 and UNS N04400 alloys. The compositions of the alloys are summarized in Table 1. Specimens with exposed surface area of 11.35 cm^2 and dimensions of 1.9 cm × 1.9 cm × 0.3 cm were polished to 600 grit using SiC paper, ultrasonically cleaned in isopropanol and air-dried. The specimens used in the crevice corrosion tests were fitted with serrated polytetrafluoroethylene (PTFE) washers (12 teeth per side) using alloy C-276 (UNS N10276) bolts isolated through PTFE sleeves and an initial torque of 0.35 Nm (50 inoz) in order to create the crevice as shown in Figure 1a. The specimens used in the synthetic seawater testing were not fitted with crevice washers.

The crevice corrosion tests were carried out in alkaline (pH 9 and 11) sodium chloride or sodium chloride + borate buffer solutions. The chloride ion concentration was varied from 0.5 mM up to 50 mM. The borate buffer solution contained 2 mM sodium hydroxide and 10.6 mM sodium tetraborate (pH ~ 9). These solutions were deaerated by purging with nitrogen gas before and during the tests.

The synthetic seawater exposures were carried out in a solution prepared according to ASTM D1141[21]. This solution was not deaerated, its oxygen content was monitored during the exposure using a handheld DO_2 meter. Free chlorine was generated in an electrochemical cell from synthetic seawater by applying 3 V direct voltage through two platinized niobium mesh electrodes for 3-10 seconds. This solution was then pumped into the test cells as shown in Figure 1b. The free chlorine levels in both the generation and test cells were monitored using a colorimetric chlorine test kit.

Electrochemical tests

The crevice stabilization and repassivation potentials were measured using cyclic potentiodynamic polarization scans in three-electrode electrochemical cells equipped with platinized niobium mesh counter electrode and saturated calomel reference electrode (SCE). Duplicate or triplicate measurements were carried out under each condition. The corrosion potential (E_{corr}) was monitored for 1 hr prior to the scan. The polarization curve was measured from -0.1 V vs. E_{corr} to a vertex current of 1 mA/cm^2 and then back to -0.1 V vs. E_{corr} at a scan rate of 0.1 mV/sec.

The synthetic seawater exposures were also carried out in three-electrode electrochemical cells. Duplicate measurements were carried out under each condition. The corrosion potential was monitored for 14 days in this case, followed by a cathodic potentiodynamic polarization scan from 0.1 V vs. E_{corr} to -1.5 V vs. SCE using a scan rate of 0.1 mV/sec. Cyclic potentiodynamic polarization curves were also measured in synthetic seawater to determine the pitting and repassivation potentials (E_{pit} and E_{rp}, respectively) using the same scan parameters as for the crevice tests.

RESULTS AND DISCUSSION

Crevice corrosion tests

The cyclic potentiodynamic polarization curves of UNS N04400 crevice specimens at different chloride levels under alkaline conditions (pH 11) are shown in Figure 2. The alloy exhibits passivity in this Cl^- concentration range, which is due to oxide growth by migration under a high electric field[6]. This oxide film is enriched in nickel[6]. The breakdown of this film is believed to occur when the chemisorbed chloride ions on the surface react with Cu, promoting its dissolution according to the following equations[10]:

$$Cu + Cl^- = CuCl + e^- \quad (2)$$

$$CuCl + Cl^- = CuCl_2^- \quad (3)$$

Under alkaline conditions, the cuprous chloride complex reacts with OH^- ions to form porous $Cu(OH)_xCl_y$ precipitates on the surface that do not exhibit barrier properties. Visual examination of the specimens revealed that the corrosion damage mainly occurred in areas just outside the crevice exposed to the bulk solution. This is due to the ennoblement of the potential in the crevice caused by the accumulation of cuprous ions[14] that occurs during the acidification of the crevice environment. According to thermodynamic calculations, Cu^+ ion is highly soluble under acidic conditions (pH $\leq$ 5)[22]. As the crevice environment becomes more acidic, the dissolution of Cu is facilitated by the solubility of Cu^+ ions, leading to their accumulation in the crevice. The crevice stabilization (i.e., passivity breakdown) and repassivation potentials decrease with increasing Cl^- concentration. The higher bulk Cl^- concentration promotes the complex formation reactions (Equations 2 and 3), therefore facilitates the Cu dissolution reaction. Addition of a pH buffer, e.g. borate, is expected to shift E_{crev} to more noble potentials thereby inhibiting the localized corrosion reaction. This effect is shown in Figure 3. E_{rcrev}, however, is not affected by the presence of the pH buffer, since the H^+ concentration is higher than the

buffer capacity of the borate solution in the environment established after the growth of the crevice. In case of the high Cu containing alloys (UNS C70600 and UNS C71500), passivity could only be achieved by the addition of borate buffer at pH 9, while they exhibited passivity without the presence of borate buffer at pH 11. UNS N04400 was passive throughout the investigated pH range without the addition of borate buffer.

Figures 4a-d show the correlation between E_{crev}, E_{rcrev} and the bulk Cl^- concentration at different temperatures for the high Cu containing alloys under mildly alkaline conditions. There is a linear relationship between the critical potentials and the logarithm of c_{Cl^-}, which can be described by the following general equation:

$$E_{crev,rcrev} = a \cdot \log c_{Cl^-} + b \quad (4)$$

where a and b are constants. This is in agreement with findings by Milosev and coworkers for the case of pitting and pit repassivation potentials of Cu-Ni alloys[10,11]. The constants and R^2 values (ratios of regression variance and total variance) determined from Equation 4 are summarized in Table 2. It is interesting to note that the crevice repassivation potential exhibits different behaviors characterized by different constants at high and low chloride levels. This is probably due to the amount of surface damage that occurs in the vicinity of the crevice as a function of chloride levels. At high c_{Cl^-}, the damage of the oxide film is more severe, thus it is harder to repassivate the surface leading to a significantly more negative E_{rcrev}. Alternatively, at low chloride ion concentrations, the water or OH^- ions can participate in the formation of the oxide layer, which is necessary for the repassivation to occur. The explanation for the critical Cl^- concentration value where the breaking point occurs is not clear at this time.

The crevice stabilization and repassivation potentials of all three alloys at different temperatures at pH 11 as a function of c_{Cl^-} are shown in Figures 5a-d. Similarly to the case discussed before, there is a linear relationship between both E_{crev} and E_{rcrev} and the logarithm of c_{Cl^-} that can be described by Equation 4. The a and b constants and R^2 values are summarized in Table 3. At this higher pH value, there is no difference between the behavior of E_{crev} and E_{rcrev} at different chloride levels. The higher OH^- concentrations give rise to easier oxide formation, thus easier repassivation, which is no longer affected by the Cl^- ion concentration.

Figure 6 shows E_{rcrev} of UNS N04400 as a function of the logarithm of c_{Cl^-} at different pH values. As expected, the crevice repassivation potentials do not significantly depend on the bulk solution pH, because the repassivation process depends on the solution chemistry developed in the crevice region during the growth of the crevice and not on the bulk solution chemistry. The difference between E_{crev} and E_{rcrev}, however, is pH dependent due to the pH dependence of E_{crev} (not shown). $\Delta E = E_{crev} - E_{rcrev}$ significantly increases with increasing pH.

The temperature dependence of E_{rcrev} of UNS N04400 at different chloride levels is summarized in Figure 7. At low c_{Cl^-}, i.e., in the range of 0.0005-0.05 M, E_{rcrev} does not depend on the temperature at moderate T. It is then significantly decreased at 95 °C. At high c_{Cl^-}, the crevice repassivation potential is linearly dependent on the temperature according to the following equation:

$$E_{rcrev} = -0.00111 \cdot T - 0.113 \qquad R^2 = 0.973 \tag{5}$$

As expected, the crevice repassivation potential decreases with increasing temperature since the corrosion process is accelerated at higher temperatures.

Effect of chlorination in synthetic seawater on corrosion potentials

The cyclic potentiodynamic polarization scans of UNS C70600, UNS C71500 and UNS N04400 alloys in synthetic seawater at room temperature are shown in Figure 8. The UNS C70600 is actively corroding under the experimental conditions. The UNS C71500 and UNS N04400 alloys exhibit passivity, the pitting and repassivation potentials increase with increasing Ni content of the alloy. These findings are in agreement with previous results that showed that in seawater with low to moderate oxygen content, the corrosion resistance of Cu-Ni alloys increased with increasing Ni content due to the higher nickel enrichment of the oxide layer at higher Ni content[5,6].

The cathodic potentiodynamic polarization curves of the alloys are shown in Figures 9a-c. Without the addition of chlorine, the cathodic current density for oxygen reduction reaction is the lowest in case of UNS C71500, and it is somewhat higher in case of the UNS C70600 and UNS N04400 alloys. This might be due to the difference in Ni enrichment of the oxide surface. When comparing the same alloy composition with and without the presence of chlorine in the solution, it is observed that the cathodic current densities do not change significantly in response to chlorination (Figures 9 b and c).

The corrosion potentials and measured dissolved oxygen levels as a function of time in case of the alloys without the presence of free chlorine are shown in Figure 10a. The dissolved oxygen concentrations were very similar for all three alloys. The corrosion potential was found to be the most negative in case of UNS C71500 and most positive in case of UNS C70600. Significant fluctuation in the corrosion potential of UNS C70600 and UNS N04400 was observed during the exposure. As shown in Figure 10b, the UNS N04400 alloy shows signs of pitting, while the significant discoloration of UNS C70600 indicates active, general corrosion of the alloy. The surface of UNS C71500 also showed some discoloration. The pits in case of the UNS N04400 specimen are shallow, which is in agreement with earlier findings by Ali and coworkers[23,24].

Figure 11a shows the corrosion potentials and dissolved oxygen concentrations in case of UNS N04400 with and without the presence of free chlorine. The dissolved oxygen concentrations were similar in case of the no free chlorine and 2 ppm free chlorine exposures. The explanation for the unusually high dissolved oxygen concentration in case of the 0.5 ppm free chlorine exposure is not known at this time. The corrosion potential remains below the repassivation potential of the alloy when no free chlorine is present. When the solution contains at least 0.5 ppm free chlorine, the corrosion potential exceeds E_{rp} for some period of time. At lower chlorine concentration, E_{corr} gradually increases from a low value to above E_{rp}, while at higher chlorine concentrations, E_{corr} reaches a very high value during the first day of exposure and then it slowly decreases below E_{rp}. Visual examination of the specimens revealed that there is significant localized corrosion damage on the surface at 2 ppm free chlorine concentration, while the least amount of pitting was observed in case of 0.5 ppm free Cl_2. Earlier research suggested that low levels of chlorine might in fact improve the corrosion resistance of Cu-Ni alloys[14]. Hypochlorite ions were also found to be beneficial by increasing the pitting potential[16]. The hypochloride ions are believed to be converted to chlorite ions that accumulate in the pores and thereby inhibit the pitting corrosion[16].

CONCLUSIONS

- In this study, correlations between the crevice corrosion parameters of selected Cu-Ni alloys and environmental conditions were established.
- In general, linear relationship was found between the logarithm of the chloride ion concentration and the crevice stabilization as well as repassivation potentials.
- There was a complex relationship between the crevice corrosion parameters and the temperature as well as the alloy composition.
- In most environments, the corrosion resistance increases with increasing nickel content.
- In synthetic seawater, chlorination has no significant effect on the cathodic behavior of the alloys.
- Higher than recommended free chlorine concentrations can lead more severe corrosion, while lower free chlorine concentrations may have a beneficial effect on the corrosion resistance of Cu-Ni alloys.
- These results provide experimental framework necessary to predict the localized corrosion susceptibility of selected Cu-Ni alloys in a thermodynamic-electrochemical model.

ACKNOWLEDGEMENTS

This work has been supported by the Department of Energy (Award No. DE-FC36-04GO14043) and co-sponsored by Chevron, DuPont, Haynes International, Mitsubishi Chemical, Shell and Toyo Engineering. The authors acknowledge the assistance provided by Mr. Carlos Lopez, Mr. Brian Derby and Mr. John E. Duck in performing the tests.

REFERENCES

1. M. S. Parvizi, A. Aladjem, J. E. Castle, International Materials Reviews (April, 1988), p. 169
2. K. M. Ismail, A. M., Fathi, W. A. Badawy, Corrosion Science (August, 2006), p. 1912
3. C. Kato, B. G. Ateya, J. E. Castle, H. W. Pickering, Journal of the Electrochemical Society (September, 1980), p. 1890
4. C. Kato, J. E. Castle, B. G. Ateya, H. W. Pickering, Journal of the Electrochemical Society, (September, 1980), p. 1897
5. R. F. North, M. J. Pryor, Corrosion Science (May 1970), p. 297
6. A. M. Zaky, F. H. Assaf, British Corrosion Journal (January, 2002), p. 48
7. G. E. McGuire, A. L. Bacarella, J. C. Griess Jr, R. E. Clausing, L. D. Hulett, Journal of the Electrochemical Society (November, 1978), p. 1801
8. V. B. Singh, A. Gupta, Journal of Materials Science (2001), p. 1433
9. K. D. Efird, Corrosion, (March, 1975), p. 77
10. I. Milosev, M. Metikos-Hukovic, Journal of the Electrochemical Society (January, 1991), p. 61
11. M. Metikos-Hukovic, I. Milosev, Journal of Applied Electrochemistry (1992), p. 448
12. I. Milosev, M. Metikos-Hukovic, Corrosion (March, 1992), p. 185
13. S. Hettiarachchi, T. P. Hoar, Corrosion Science (July, 1979), p. 1059
14. W. Schleich, "Application of Copper-Nickel Alloy UNS C70600 for Seawater Service", CORROSION/2005, paper no. 05222 (Houston, TX: NACE, 2005)

15. M. de Romero, Z. Duque, O. de Rincon, O. Perez, I. Araujo, A. Martinez, Corrosion (August, 2000), p. 867
16. V. K. Gouda, A. A. Khedr, A. M. Fathi, A. M., Bulletin of Electrochemistry (July, 2000), p. 289
17. N. Sridhar, G. A. Cragnolino, Corrosion (December, 1993), p. 967
18. A. Anderko, N. Sridhar, D. S. Dunn, Corrosion Science (July, 2004), p. 1583
19. A. Anderko, R. D. Young, Corrosion (May, 2000), p. 543
20. A. Anderko, P. McKenzie, R. D. Young, Corrosion (March, 2001), p. 202
21. ASTM D114-98 "Standard Practice for the Preparation of Substitute Ocean Water, ASTM International, 2003
22. OLI Stream Analyzer 2.0, OLI Systems, 2006
23. A. J. Ali, J. R. Ambrose, Corrosion Science (July, 1992), p. 1147
24. A. J. Ali, Corrosion Science (April, 1994), p. 773

TABLES AND FIGURES

TABLE 1
COMPOSITIONS OF ALLOYS INVESTIGATED (WEIGHT %)

	Cu	Ni	Fe	Mn	C	Si	Trace elements to balance
UNS C70600	88.75	9.90	1.27	0.44	0.006	-	P, Pb, S, Zn
UNS C71500	67.89	30.85	0.66	0.49	0.014	-	P, S, Zn
UNS N04400	32.85	63.92	2.03	0.80	0.125	0.08	Al, Pb, S, Zn, Co, P, Sn

TABLE 2
COEFFICIENTS AND R^2 VALUES OF E_{CREV} AND E_{RCREV} VS. LOG [Cl^-] EQUATIONS FOR UNS C70600 AND UNS C71500 AT pH 9

E_{crev}, 23°C

Alloy	***a***	***b***	**R^2**
UNS C70600	-0.0604	-0.138	0.913
UNS C71500	-0.0612	-0.059	0.834

E_{rcrev}, 23°C

Alloy	***a***	***b***	**R^2**
UNS C70600, low [Cl^-]	N/A	N/A	N/A
UNS C70600, high [Cl^-]	-0.0083	-0.089	0.966
UNS C71500, low [Cl^-]	-0.0479	-0.00046	N/A
UNS C71500, high [Cl^-]	-0.0114	-0.109	0.945

E_{crev}, 60°C

Alloy	***a***	***b***	**R^2**
UNS C70600	-0.0239	-0.190	0.824
UNS C71500	-0.0555	-0.256	0.882

E_{rcrev}, 60°C

Alloy	***a***	***b***	**R^2**
UNS C70600, low [Cl^-]	-0.0359	-0.438	0.979
UNS C70600, high [Cl^-]	-0.0064	-0.302	N/A
UNS C71500, low [Cl^-]	N/A	N/A	N/A
UNS C71500, high [Cl^-]	-0.0181	-0.253	0.771

TABLE 3
COEFFICIENTS AND R^2 VALUES OF E_{CREV} AND E_{RCREV} VS. LOG [Cl^-] EQUATIONS FOR UNS N04400, UNS C70600 AND UNS C71500 AT pH 11

E_{crev}, 23°C

Alloy	***a***	***b***	**R^2**
UNS N04400	-0.0201	0.0015	0.974
UNS C70600	-0.0284	-0.286	0.917
UNS C71500	-0.0156	-0.160	0.925

E_{rcrev}, 23°C

Alloy	***a***	***b***	**R^2**
UNS N04400	-0.01198	-0.133	0.903
UNS C70600	-0.0284	-0.286	0.917
UNS C71500	-0.0156	-0.160	0.925

E_{crev}, 60°C

Alloy	***a***	***b***	**R^2**
UNS N04400	-0.0389	-0.188	0.938
UNS C70600	-0.0667	-0.565	0.753
UNS C71500	-0.0435	-0.212	0.897

E_{rcrev}, 60°C

Alloy	***a***	***b***	**R^2**
UNS N04400	-0.0153	-0.194	0.874
UNS C70600	-0.0256	-0.243	0.899
UNS C71500	-0.0135	-0.276	0.866

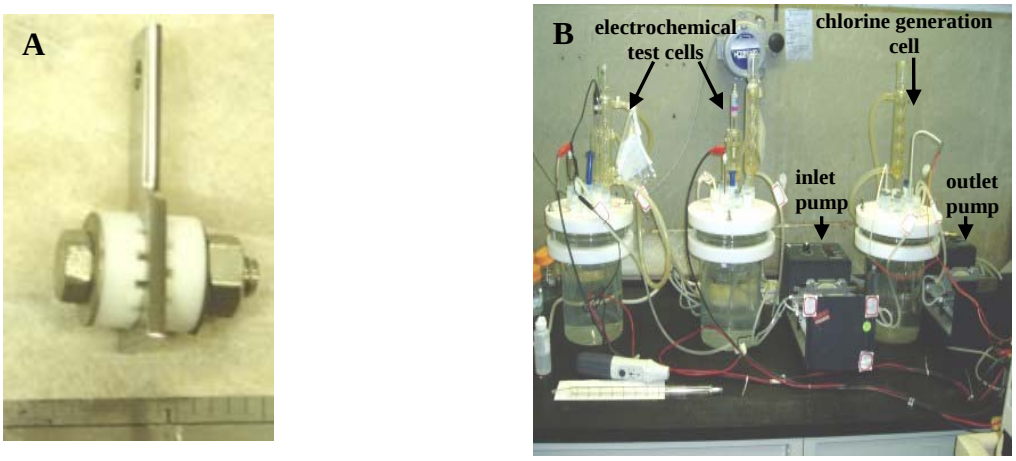

FIGURE 1 – A: Geometry of specimen used in crevice corrosion tests. B: Electrochemical cells used in chlorinated seawater exposures.

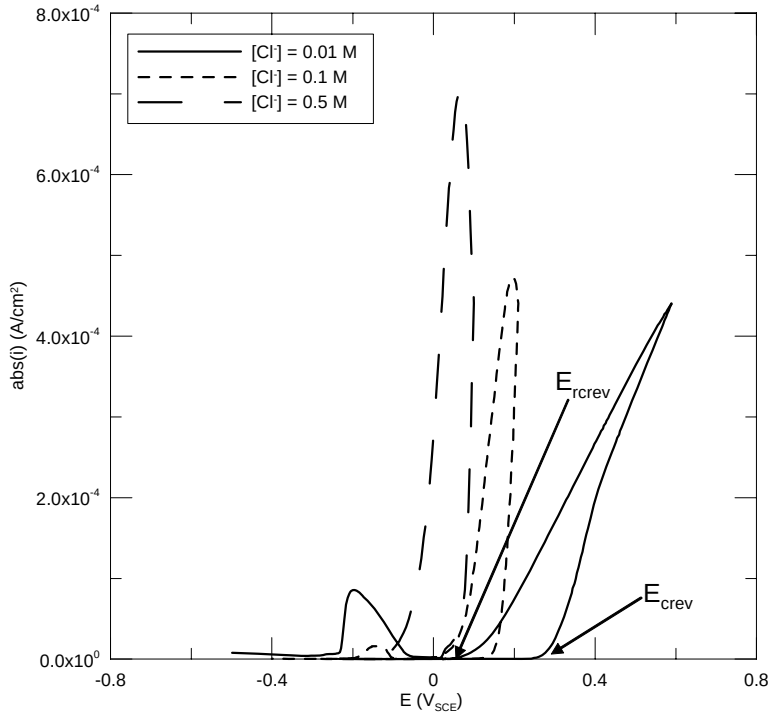

FIGURE 2 – Cyclic potentiodynamic polarization curves of UNS N04400 as a function of chloride ion concentration at room temperature under alkaline conditions (pH 11).

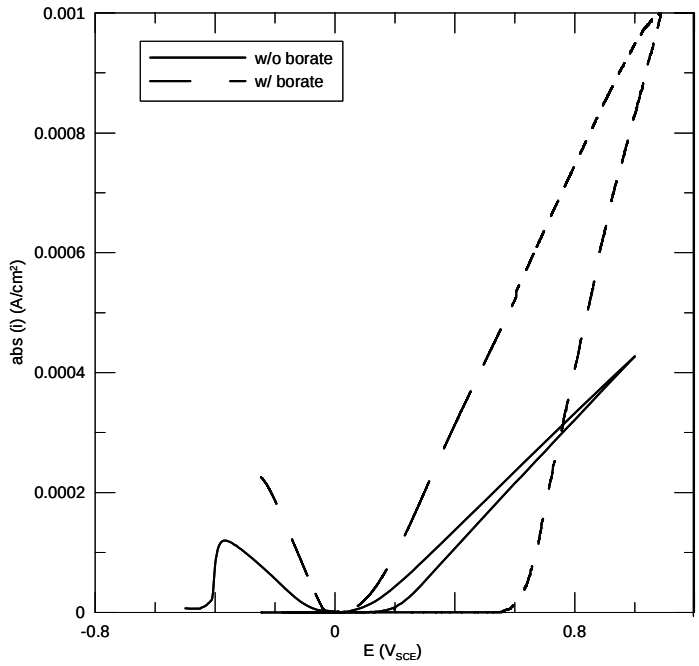

FIGURE 3 – Cyclic potentiodynamic polarization curves of UNS N04400 in pH 9, 0.005 M chloride solution with and without the presence of borate buffer.

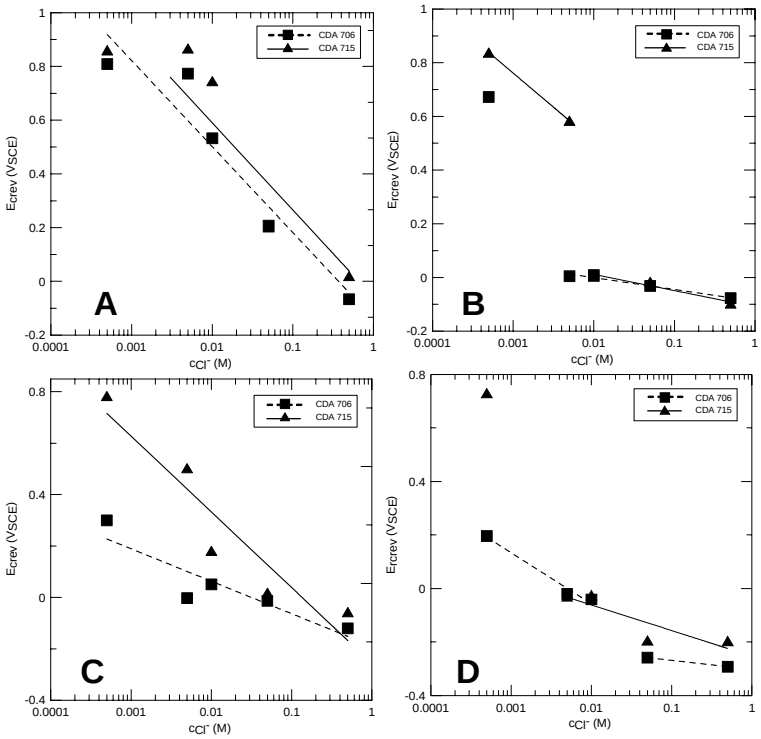

FIGURE 4 – UNS C70600 and UNS C71500 in pH 9 borate buffer solution containing chloride ions; A: E_{crev} as a function of [Cl^-] at 23°C; B: E_{rcrev} as a function of [Cl^-] at 23°C; C: E_{crev} as a function of [Cl^-] at 60°C; D: E_{rcrev} as a function of [Cl^-] at 60°C.

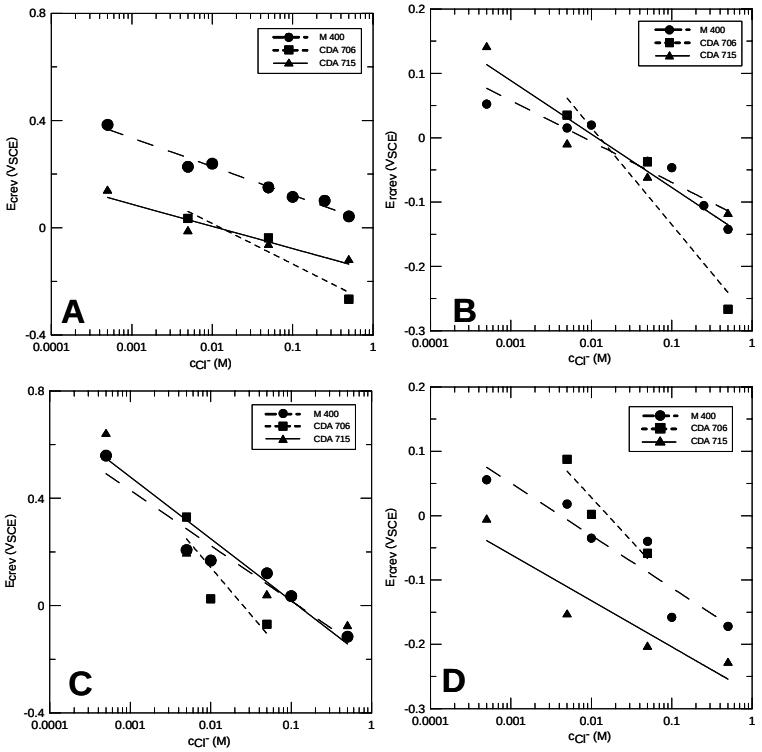

FIGURE 5 – UNS N04400, UNS C70600 and UNS C71500 in pH 11 sodium chloride solutions; A: E_{crev} as a function of [Cl^-] at 23°C; B: E_{rcrev} as a function of [Cl^-] at 23°C; C: E_{crev} as a function of [Cl^-] at 60°C; D: E_{rcrev} as a function of [Cl^-] at 60°C.

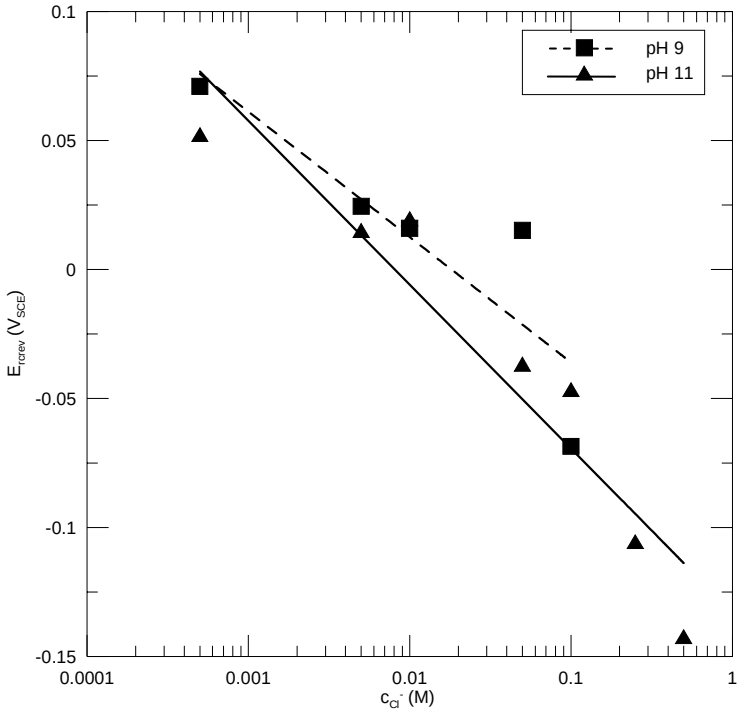

FIGURE 6 – Crevice repassivation potential of UNS N04400 at room temperature as a function of chloride ion concentration and solution pH in alkaline sodium chloride solutions.

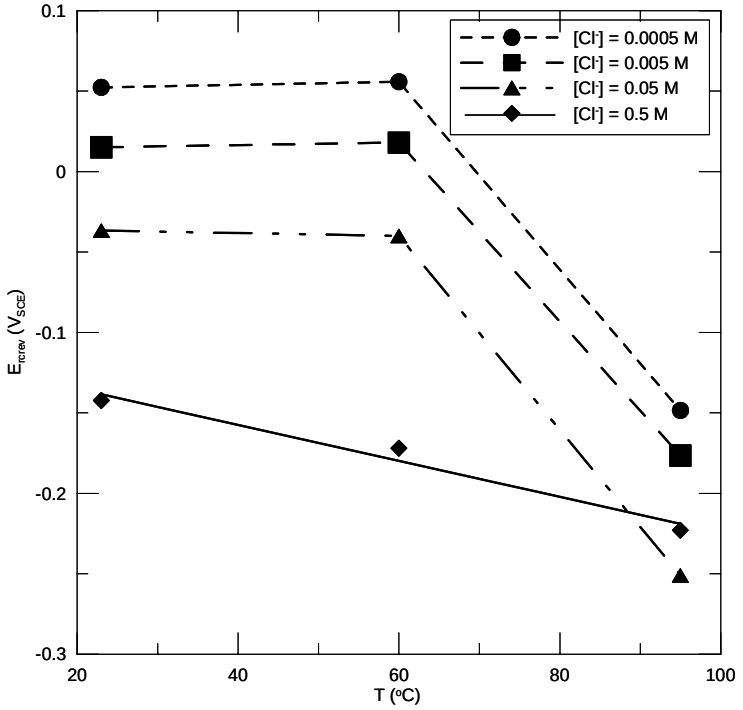

FIGURE 7 – Crevice repassivation potential of UNS N04400 as a function of temperature and chloride ion concentration in pH 11 sodium chloride solution.

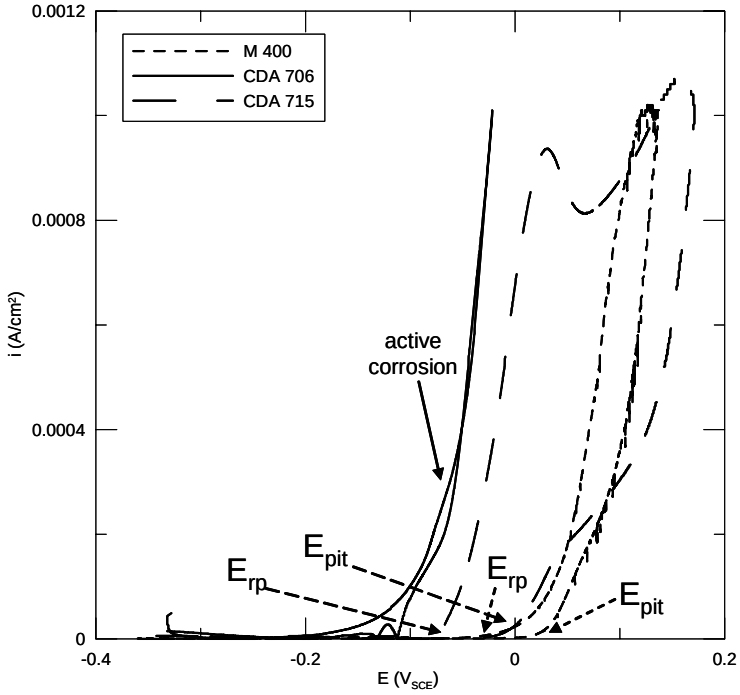

FIGURE 8 – Cyclic potentiodynamic polarization scans of UNS N04400, UNS C70600 and UNS C71500 alloys in synthetic seawater at room temperature.

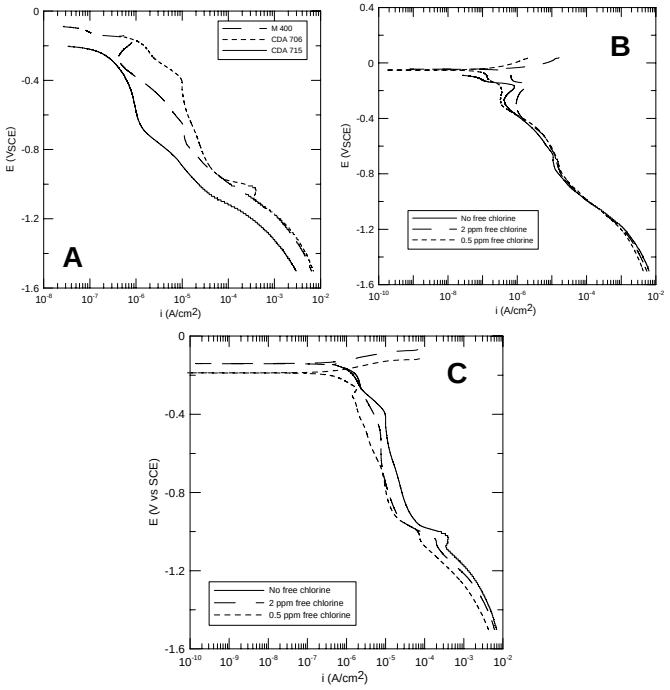

FIGURE 9 – Cathodic potentiodynamic polarization curves of
A: UNS N04400, UNS C70600 and UNS C71500 after 14 days of exposure to synthetic seawater at room temperature; B: UNS N04400 after 14 days of exposure to synthetic seawater at different chlorine levels at room temperature; C: UNS N04400 after 14 days of exposure to synthetic seawater at different chlorine levels at room temperature.

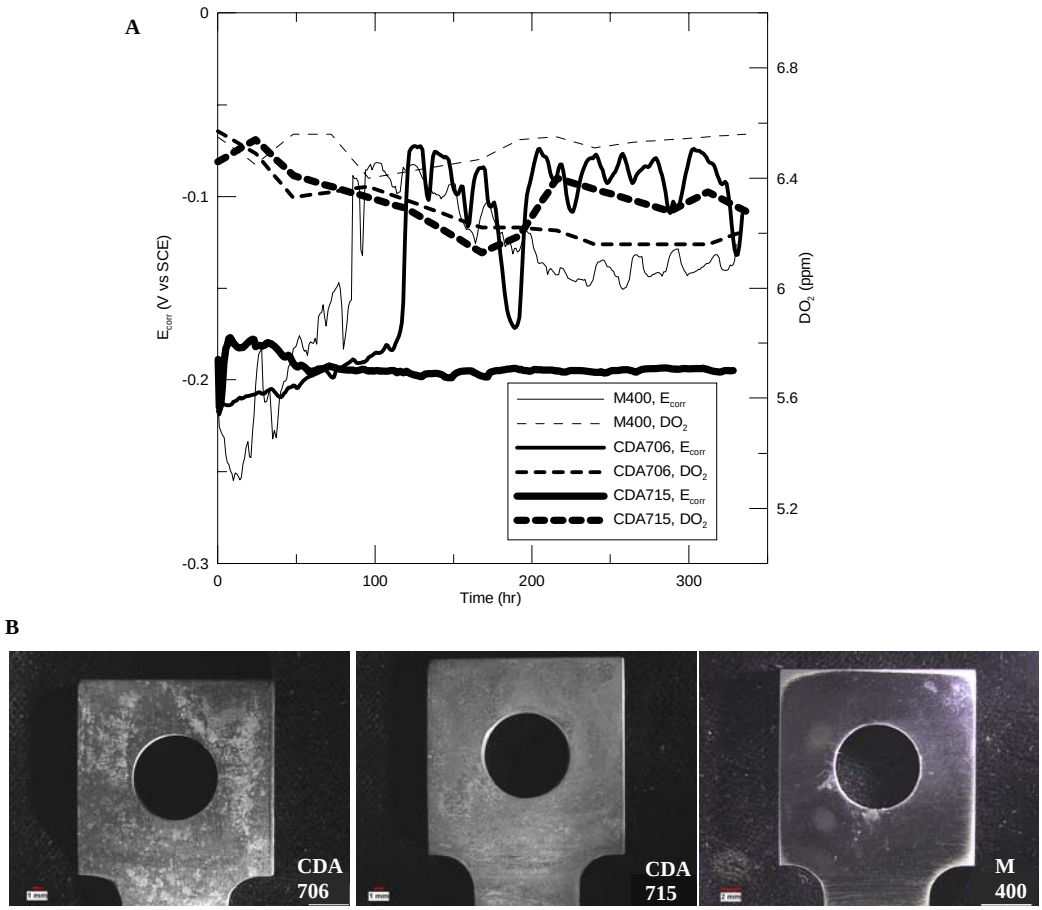

FIGURE 10 – A: Corrosion potential of UNS N04400, UNS C70600 and UNS C71500 as a function of exposure time in synthetic seawater, as well as dissolved oxygen concentrations measured in the solutions. B: Low magnification optical microscope images of UNS N04400, UNS C70600 and UNS C71500 alloys exposed to synthetic seawater for 14 days.

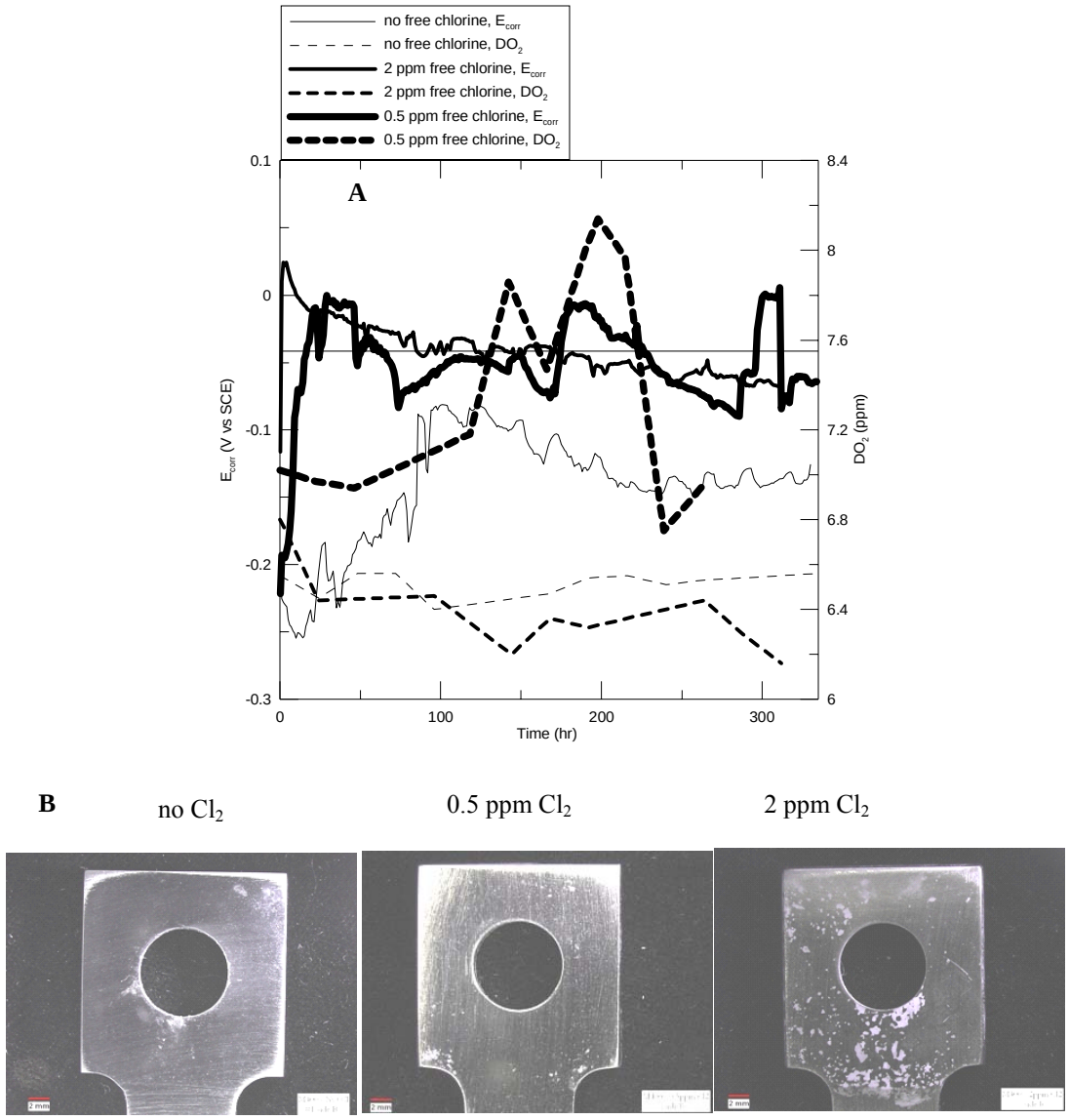

FIGURE 11 – A: Corrosion potential of UNS N04400 as a function of exposure time in synthetic seawater containing different concentrations of free chlorine, as well as dissolved oxygen concentrations measured in the solutions. B: Low magnification optical microscope images of UNS N04400 exposed to synthetic seawater containing different free chlorine concentrations for 14 days.